Evaluation of low-kV energy X-ray radiation effect on breast cancer cells incubated with gold nanoparticles capped with aminolevulinic acid, methyl aminolevulinate, and gamma-aminobutyric acid

Isabela Santos Lopes[b], Noemy Rodrigues Santos[a], Giovana Dias da Silva[a], Daniel Perez Vieira[a], Lilia Coronato Courrol[b]

[a]Centro de Biotecnologia, Instituto de Pesquisas Energéticas e Nucleares, São Paulo, São Paulo, Brazil

[b]Instituto de Ciências Ambientais, Químicas e Farmacêuticas, Departamento de Física, Universidade Federal de São Paulo, Diadema, São Paulo, Brazil

*Corresponding author: lcourrol@unifesp.br

Abstract

Gold nanoparticles (AuNPs) have unique properties, including size-dependent optical and electronic characteristics, biocompatibility, and ease of functionalization, making them attractive for various diagnostic and therapeutic applications. The goal of this work was to verify the potential application of gold nanoparticles capped with aminolevulinic acid (ALA), methyl aminolevulinate (MALA), and gamma-aminobutyric acid (GABA) in low-energy X-ray diagnostics and therapy of breast cancer. ALA and MALA induce the accumulation of protoporphyrin IX (PpIX) in cancer cells. PpIX, in turn, can be excited by Cherenkov radiation, producing reactive oxygen species after energy or electron transfer from the triplet excited state of PpIX to molecular oxygen, which induces cell death by apoptosis or necrosis. The results indicated that ALA and MALA nanoparticles promoted reduced cell viability by approximately 20% with X-ray irradiation at an energy level of 35 kV for 5 minutes. Breast cancer cells possess GABA receptors, allowing for targeted effects by GABANPs, which can enhance contrast and improve diagnostic potential. GABAAuNPs also demonstrated decreased cell viability in ~10% following X-ray irradiation, making them a promising material for both breast cancer diagnosis and treatment.

Keywords: Breast cancer, gold nanoparticles, aminolevulinic acid, methyl aminolevulinate, and gamma-aminobutyric acid.

1. Introduction

Breast cancer stands as the most prevalent form of cancer affecting women on a global scale. According to data from the World Health Organization (WHO), in 2020, approximately 2.3 million women received diagnoses of breast cancer, resulting in 685,000 deaths globally(2019). The main known subtypes are grouped into four categories: Luminal A, Luminal B, human epidermal growth factor receptor positive (HER2+), and triple-negative (TNBC), dependent on expression of hormone receptors: estrogen receptor-positive (ER+), progesterone receptor positive (PR+), human epidermal growth factor receptor positive (HER2+). The Luminal A (ER+, PgR-/+, HER2-) subtype expresses hormonal receptors with low proliferative activity, while the

Luminal B (ER+, PgR-/+, HER2+/-) subtype has higher proliferative activity and a challenging prognosis. HER2+ (ER+, PgR-/+, HER2+) tumors are aggressive and require targeted therapies, whereas TNBC (ER-, PgR-, HER2-) is heterogeneous and aggressive, demanding diverse therapeutic approaches(Hon *et al.*, 2016).

Early identification plays a vital role in enhancing treatment results in the initial phases of breast cancer. Mammography is the most commonly employed imaging method for breast cancer screening and diagnosis, reducing mortality rates (Swaminathan *et al.*, 2023). The American Cancer Society advises women to commence annual mammograms at 40 years old. Mammography machines typically operate in the range of 25 kV to 35 kV, and 35 kV is a commonly used energy setting for breast imaging. At the low energies typically used for mammographic X-ray images, gold nanoparticles (AuNPs) exhibit remarkable attenuation, even at very low concentrations. AuNPs have been exploited as contrast agents, which enables high resolution (Torrisi *et al.*, 2019).

Breast cancer treatment can be categorized into local treatment through surgery, radiotherapy, and systemic treatment via chemotherapy, hormone therapy, and biological therapy(Noor *et al.*, 2021). The selection of treatment options depends on the disease's stage and the tumor's characteristics (Akram *et al.*, 2017).

X-ray radiotherapy is a standard and effective treatment for various cancers, but it affects both tumors and healthy tissues, resulting in potential damage and side effects(Janssen *et al.*, 2018). Efforts are being made to optimize radiotherapy to minimize these adverse effects and enhance cell survival in healthy tissue. The importance of optimizing radiation dose delivery processes to increase the efficacy of radiotherapy and minimize the dose required for tumor death is evident. One promising avenue is using AuNPs, which come in different shapes and sizes and have shown promise in drug delivery, imaging applications, and photothermal therapy(Allen *et al.*, 2022; Amina and Guo, 2020). In breast cancer management, gold nanoparticles have been investigated for their potential to enhance radiotherapy dose (Fathy *et al.*, 2018; Akter *et al.*, 2023). The surface of these nanoparticles can be functionalized with various biomolecules, enabling target selectivity. Nanoparticles designed for radio enhancement can heighten the susceptibility of cancer cells to radiation(Bilynsky *et al.*, 2022). When subjected to ionizing radiation, such as X-rays, gold nanoparticles have the potential to amplify the radiation dosage targeted at cancer cells, thus reducing harm to adjacent healthy tissue and augmenting the overall efficacy of therapy (Chen *et al.*, 2020).

Aminolevulinic acid (ALA) gold nanoparticles have been studied, proving their theranostic applications(Goncalves *et al.*, 2015; Goncalves *et al.*, 2020). Combined with ALA, these nanoparticles cause a preferential accumulation of protoporphyrin IX (PpIX) in cancerous cells compared to normal cells. This difference in metabolism between normal and tumor cells allows for ALAAu-based photodynamic diagnosis and therapy. By transporting ALAAuNPs to specific cells, the diagnostic and radiotherapy dose can be significantly enhanced.

Methyl-5-aminolevulinate (MALA) is another compound like ALA used in clinical settings(Blanco *et al.*, 2015; Mateus *et al.*, 2014). Due to its methyl group, MALA is more selective for tissues and offers better results in photodynamic therapy (PDT) sine increase PpIX content inn cells in comparison with ALA (Goncalvez *et al.*, 2018).

The neurotransmitter gamma-aminobutyric acid (GABA), well-known for its role in the central nervous system, has also been found to be altered in cancer cells, particularly in breast cancer(Brzozowska *et al.*, 2017). Research has indicated that the stimulation of GABA receptors

has the potential to suppress both the growth and spread of tumor cells (Yang *et al.*, 2023). Numerous studies have indicated that individuals who exhibit higher GABA levels tend to experience more positive outcomes in terms of disease-free survival and overall survival when compared to those with lower GABA levels (Wu *et al.*, 2023; Yang *et al.*, 2023).

This study describes the GABAAuNPs synthesis for the first time, employing the photoreduction process. ALA, MALA, and GABA gold nanoparticles were employed in an *in-vitro* low-energy X-ray therapy.

2. Experimental

2.1. AuNPs synthesis

Tetrachloroauric acid ($HAuCl_4$), 5-aminolevulinic acid, Methyl δ-aminolevulinate, and gamma-aminobutyric acid were purchased from Sigma-Aldrich.

To prepare the ALAAuNPs, MALAAuNPs, GABAAuNPs, 45 mg of ALA/MALA/GABA, 15 mg of $HAuCl_4$ and 100 mg of Polyethylene glycol 10000 (PEG) were diluted in 100 mL of distilled water and followed by vigorous stirring for 5 minutes. ALA, MALA and GABA solutions (10 mL) were illuminated for 2, 5 and 3 min, respectively, with a 300 Watts Xenon lamp from Cermax, with an intensity estimated to be 3.6 W/cm ^{2}.

All solutions have the pH adjusted to ~ 7.0 after NaOH solution irradiation.

2.2. Nanoparticle characterization

The UV-Vis absorption spectra were measured using a Shimatzu spectrophotometer with 1 cm quartz cells.

The shape and sizes of the AuNPs were determined using transmission electron microscopy (TEM) with a JEM-2100 Jeol instrument (Zeiss, Germany) at Laboratory of Microscopy and Microanalysis (LMM) is a multi-user laboratory, located at the Center for Science and Technology of Materials (CCTM) of the Institute of Energy and Nuclear Research (IPEN).

The surface charges on the nanoparticles were measured using Zeta potential analysis, conducted with the Malvern Instruments Zetasizer (Worcestershire, UK) and the DKSH ZetaView at the multi-user laboratory from the Federal University of ABC.

FTIR spectra were recorded using a Shimadzu Prestige-21 spectrometer (Shimadzu Corp., Kyoto, JP) with a resolution of 2 cm^{-1} within the range of 4000 cm^{-1} to 400 cm^{-1}.

2.3. Cytotoxicity test

The MCF-7 breast tumor cells were cultured in RPMI 1640 medium supplemented with 10% fetal bovine serum (FBS) and 1% penicillin/streptomycin at 37°C with 5% CO_2. Cells were sub-cultured every 3 days at 70-80% confluency and harvested using 0.25% trypsin.

For the cytotoxicity analysis $8x10^3$ cells/well were plated in 96-well flat-bottom plates and incubated for 24 h for adhesion and growth. Afterward, the cells were divided into different groups and incubated with ALAAu, MALAAu, and GABAAu at concentrations of 5% (475 µL

culture medium + 25 µL of NPs), 4% (480 µL culture medium + 20 µL of NPs), 3% (485 µL culture medium + 15 µL of NPs), and 2% (490 µL culture medium + 10 µL of NPs).

The plates were then incubated for 48 h at 37°C with 5% CO_2. After incubation, the supernatant was removed, and the cells were washed with PBS before being incubated for another 24 h in RPMI medium.

Cell viability was assessed using the 3-(4,5-dimethylthiazol-2-yl)-5-(3-carboxymethoxyphenyl)-2-(4-sulfophenyl)-2H-tetrazolium, MTS (CellTiter 96® AQueous MTS Reagent). The absorbance at 490 nm was measured and is directly proportional to the number of live cells in the culture. The results were statistically compared using ANOVA and the Dunnett test against negative controls (NaCl 5%) or positive controls (DMSO 10%). The percentage of cell viability was calculated after background absorbance correction and blank absorbance subtraction as follows:

% Cell viability = 100 x (Experimental well absorbance/untreated control well absorbance).

2.4. Quantification of PpIX fluorescence by Hight Content Screening (HCS)

The High Content Screening (HCS) quantification assay was carried out in collaboration with the Genetics and Molecular Hematology Laboratory, Hospital das Clínicas, Faculty of Medicine, University of São Paulo, USP.

The assay was performed in 96-well plates (Cornig) with $2x10^4$ cells/well. The cells were maintained for 24 h in an oven (37°C and 5% CO_2) for adhesion. Subsequently, the culture medium was replaced with a nanoparticle solution (10 µL of ALAAu and MALAAu in 40 µL of culture medium), which was then subjected to a 24 h incubation in an oven. Following this exposure period, the cells underwent a PBS wash and a 1 µL/well application of Hoechst 3342 fluorescence dye (at a 1/100 dilution). For each well, nine sites were imaged, and this process was repeated in three separate wells for each treatment. Cells displaying PpIX fluorescence were identified using the cell scoring functionality within the MetaXpress software.

2.7. Radiotherapy procedure

After analyzing the results obtained from the serial dilution, the concentrations for the treatment were selected. The experiment was conducted using two plates - one for irradiated samples and the other as a control plate.

Studied groups:

A. Cell control (CC) - n=32

B. Negative control: 5% NaCl solution - n=8 (Total volume = 1000 µL, comprising 950 µL of culture medium + 50 µL of NaCl)

C. Positive control: 10% DMSO solution - n=8 (Total volume = 1000 µL, comprising 900 µL of culture medium + 100 µL of DMSO)

D. ALAAuNPs, MALAAuNPs, GABAAuNPs (n=8 for each group). The concentration of NPs used in this experiment did not induce cytotoxicity.

Experimental Timeline:

Day 1: Cells were plated in a 96-well plate at a density of 5000 cells per well. The plate was then incubated at 37°C in a 5% CO_2 atmosphere for 48 h to allow for adhesion and growth.

Day 2: After 48 h, the culture medium in the wells was replaced with 100 µL of the respective nanoparticles solutions at their proper concentrations. The plate was again incubated at 37°C with 5% CO_2 for 24 h.

Day 3: After the 24 h incubation, the wells were washed with 100 µL of PBS. Then, 20 µL of PBS per well was added to prepare the samples for irradiation. The plates were positioned vertically one meter away from the beam exit, as per the specified norms, within the radiation field of 12 cm diameter, aided by calibrated lasers. The X-ray beam quality simulating the energy range of a mammography device was used. The radiation reference for mammography was implemented in the Pantak/Seifert system, traceable to the German primary laboratory, Physikalisch-Technische Bundesanstalt (PTB). The parameters for the quality RQR - 4M are listed in Table 1.

Table 1 - Parameters and quality implemented in the Pantak/Seifert system.

Quality	kV	mA	CSR (mmAl)	Filtration (mm)	kerma rate (mGy/min)
RQR - 4M	35	10	0.41	0.07 Mo	19.2

An X-ray camera using the Radcal RC6M Series ionization chamber was employed to determine the X-ray beam characteristics. The camera was calibrated in the PTB with a measurement uncertainty of ± 0.96%, and the Keithley 6517A Electrometer was used with an uncertainty of ± 2.0% (Standard IEC61267). The camera was positioned at 1m from the source, with collimators measuring 34 mm and 50.8 mm and a field diameter of 12 cm.

The plate was irradiated for 5 min, resulting in a entry dose of approximately 96 mGy. The control plate underwent the same conditions as the irradiated plate for comparison purposes.

After irradiation, the wells were washed, and 100 µL of culture medium per well was added. The plate was incubated at 37°C within an atmosphere containing 5% CO_2 for a duration of 24 h.

4th day: After 24 h of incubation, the wells were washed with PBS. A solution consisting of 2 mL of MTS, 100 µL of phenazine methosulfate (PMS), and 9.9 mL of culture medium was prepared. Then, 100 µL of the prepared solution was added per well.

After a 2 h incubation period, the spectrophotometer was used to measure the readings.

Statistical Analysis

All studies were performed in triplicate. The results were statistically compared (ANOVA and Dunnett test) with controls.

3. Results *Nanoparticles characterization*

The absorbance spectra of the ALAAu, MALAAu, and GABAAu nanoparticles are shown in Fig. 1a. The ALAAuNPs and MALAAuNPs presented the SPR (surface plasmon resonance) peak around 544 nm. In contrast, GABAAuNPs presented the SPR band at ~ 521 nm.

Figure 1b shows the TEM images of gold nanoparticles. ALAAu e MALAAu are spherical, but GABAAuNPs present a worm-like shape.

Figure 1c shows the FTIR of the study nanoparticles, demonstrating some similarities in the spectra and presence of amino acids in the nanoparticles' surface. The data indicate that the synthesis mechanism of gold nanoparticles with the three different ligands occurred similarly.

Table 1 compares the Zeta potential and polydispersity index of the ALAAu, MALAAu, and GABAAu nanoparticles. Similar values were found. The nanoparticles have negative surface charges and similar stabilities.

Table 1. Zeta potential and polydispersity parameters of ALAAu, MALAAu, and GABAAu nanoparticles.

Parameter	ALAAu	MALAAu	GABAAu
Zeta potential (mV)	-23.1±1.0	-21,9 ± 0,98	-25.1±2.0
PDI	0.483	0.437	0.333

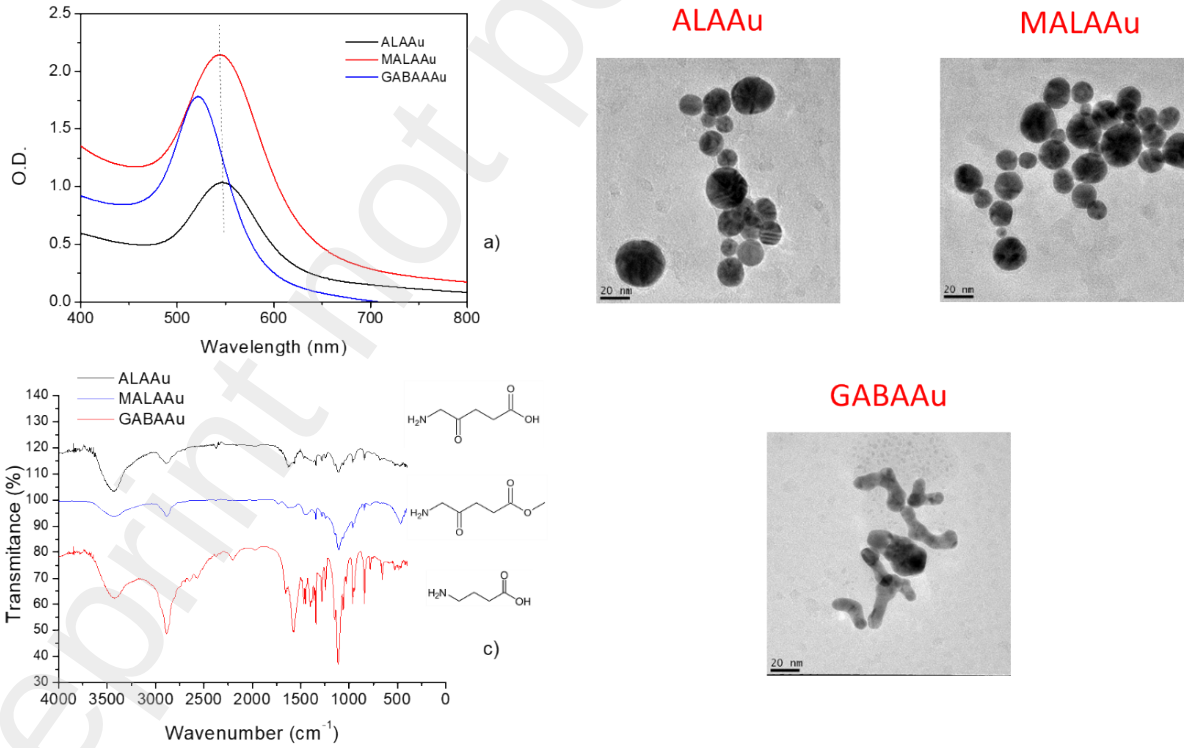

Figure 1. a) UV-Vis spectra; b) TEM images and c) FTIR of ALAAu, MALAAu and GABAAuNPs.

3.2. Cytotoxicity study

The cytotoxicity effects of ALAAu, MALAAu and GABAAu nanoparticles in MCF-7 cells can be observed in Figure 2, where the percentage of cell viability is plotted in function of the percentage of nanoparticles present in the culture medium added in each well. The results showed that ALAAuNPs and MALAAuNPs presented toxicity at 4 and 5% concentrations, but GABAAuNPs did not present toxicity in the studied concentrations.

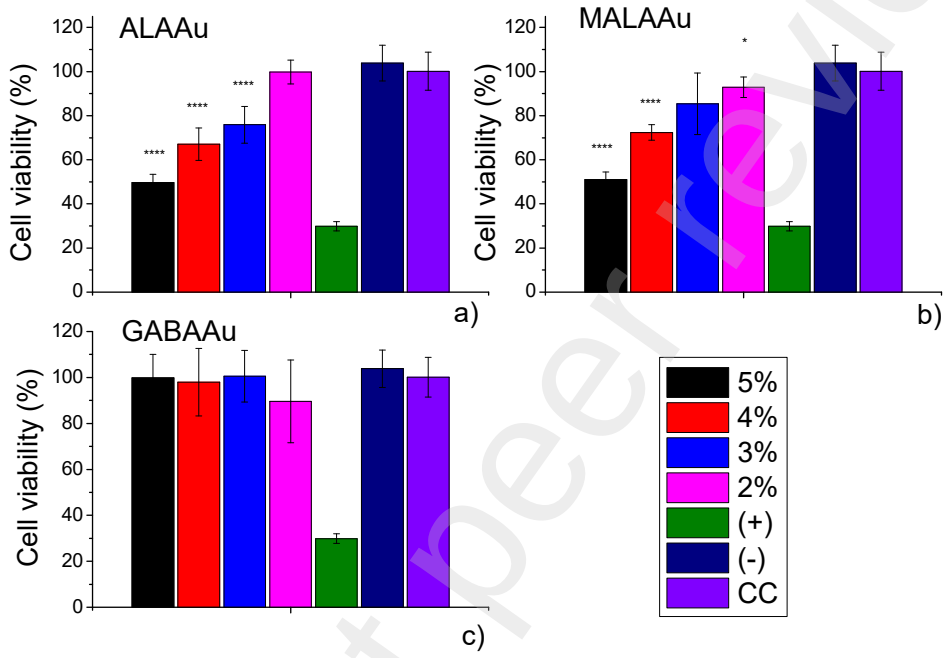

Figure 2. Cell viability test in MCF-7 lineage, incubated for 24 h with a) ALAAu, b) MALAAu and c) GABAAuNPs. Data were compared using the ANOVA test followed by the Dunnett test, with p (****): p-value < 0.0001, (*):p-value<0.01.

3.3. PpIX fluorescence

ALAAu/MALAAu uptake and its subsequent transformation into PpIX within the cellular environment was monitored by PpIX fluorescence analysis performed by High Content Screening in breast tumor cells. In the obtained images, shown in Fig. 3, it is possible to see the PpIX fluorescence in red, inside the cells. The cells were also stained with the fluorescent dye Hoechst 3342, which marks in blue all viable cells. In the control group, the cell nuclei exhibited distinct blue staining with no detectable red emission visible in the imagery. However, in the presence of nanoparticles, a decrease in the cell count was noted, and some cells displayed a noticeable red emission, indicative of the conversion to PpIX. It was observed that cells treated with ALAAu or MALAAu, presented an increased concentration of PpIX in comparison with control cells.

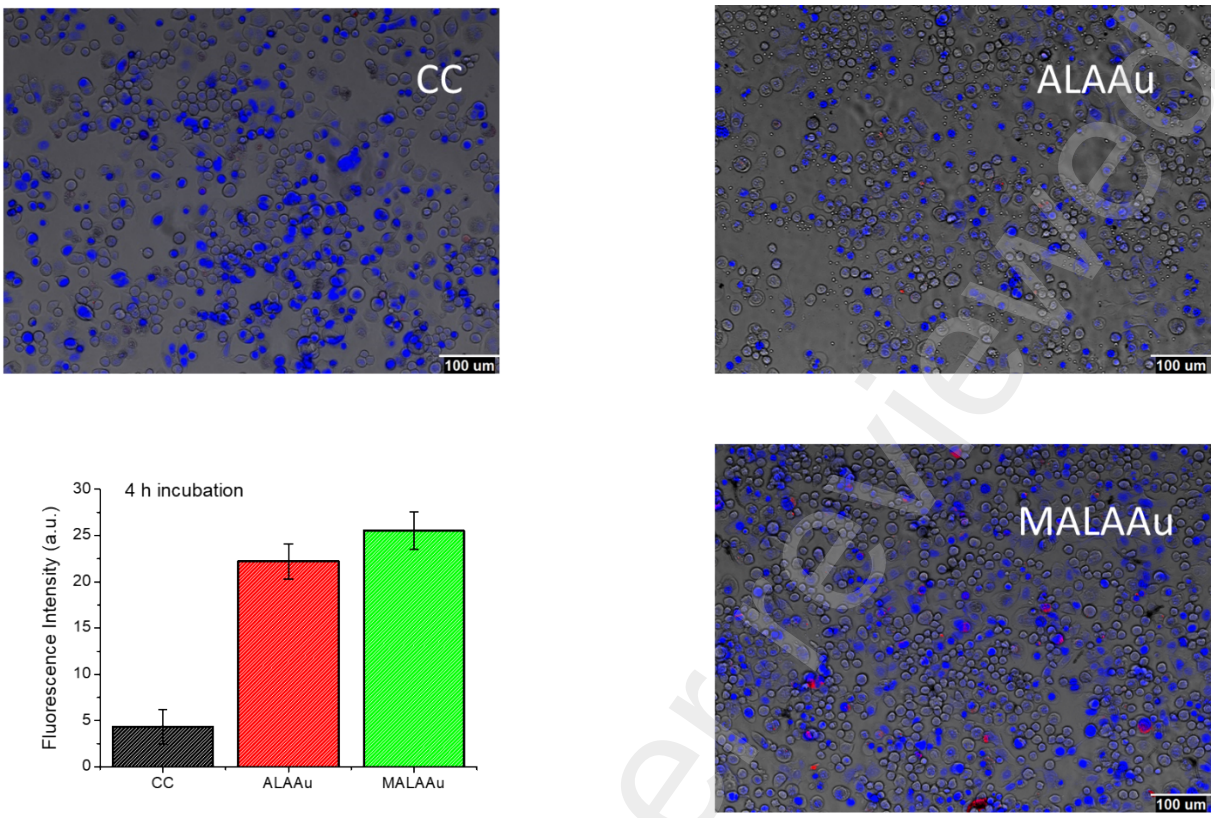

Figure 3. HCS images obtained of MCF-7 cells and cells incubated for 4 h with ALAAuNPs and MALAAuNPs. The cells were stained with Hoechst 3342, 2 h before imaging. The PpIX presents fluorescence in the red region around 675 nm. The graph compares PpIX fluorescence intensities.

3.4. X-ray irradiation

The results obtained from irradiating MCF-7 for 5 min with 35KV X-rays are shown in Fig. 4. The results demonstrated that the irradiation of cells incubated with ALAAuNPs and MALAAuNPs reduced cell viability by approximately 22.9% and 18.7%, respectively, when compared to non-irradiated cell groups (p-values<0.0001). The combination of GABAAuNPs and X-ray irradiation resulted in a decrease in cell viability of about 9.7%, with was statistically significant (p-value < 0.01) when compared to non-irradiated cells. Control group and positive and negative controls exhibited no changes during the 5-minute irradiation period.

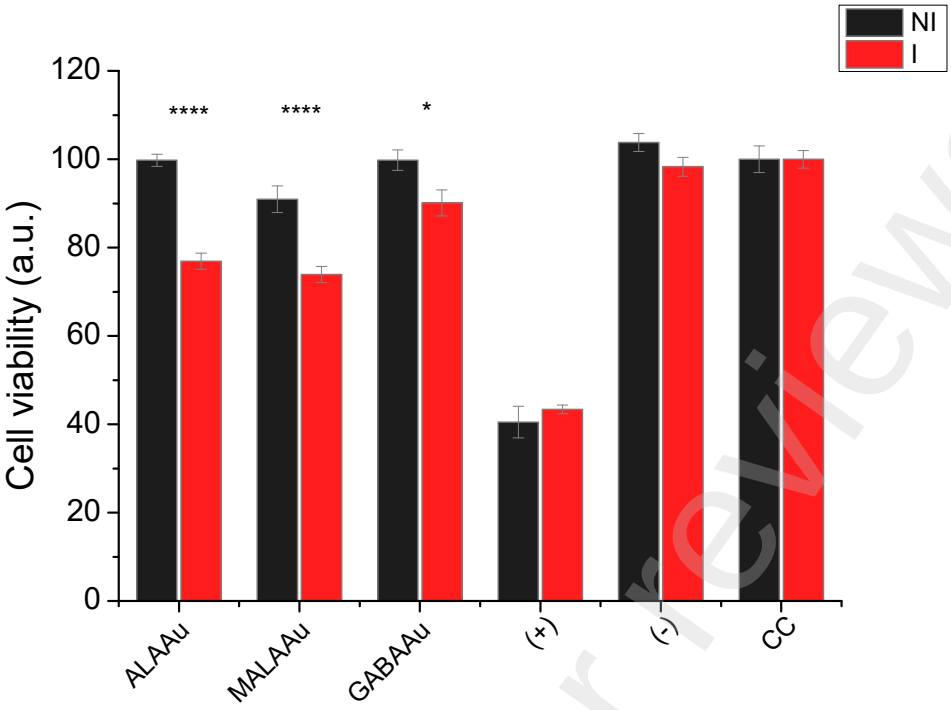

Figure 4. MCF-7 viability after incubation with ALAAu, MALAAu, and GABAAu for 24 h not irradiated and irradiated with low-energy X-rays. Data were compared using the ANOVA test followed by the Dunnett test. (****): p-value < 0.0001, (*):p-value<0.01.

4. Discussion

Mammograms are generally considered safe; however, like all medical procedures involving radiation, they expose the breast to low X-rays(Diffey, 2017). Nonetheless, the benefits of early breast cancer detection through mammography far outweigh the potential risks for most women.

Utilizing low-dose X-rays generates detailed images of breast tissues, enabling early detection and prevention of breast cancer even before physical symptoms arise(Lebron-Zapata and Jochelson, 2018). In contrast to screening mammography, diagnostic mammograms provide more in-depth and targeted assessments. They are carried out when a woman experiences a mass, breast discomfort, discharge from the nipple, or abnormalities found during a screening mammogram(Schulz-Wendtland *et al.*, 2009). Diagnostic mammography allows for a closer examination of breast tissues to determine the nature of any detected abnormality(Perry *et al.*, 2019).

Several contrasts are involved in mammography, which plays a crucial role in interpreting the images and detecting abnormalities(Perry *et al.*, 2019). These contrasts refer to the differences in appearance between various types of tissues within the breast, and they are essential for distinguishing normal breast structures from potentially suspicious or cancerous lesions(Lorente-Ramos and Arman, 2022).

Gold nanoparticles have gained interest in breast mammography due to their unique properties and potential applications(Chen *et al.*, 2022). They can interact with X-rays, making

them promising contrast agents for enhancing the detection and diagnosis of breast cancer in mammography(Hsu *et al.*, 2020).

Gold nanoparticles can enhance the contrast between malignant and adjacent healthy tissue on mammograms. This effect is primarily attributed to the high atomic number of gold (Au) and its ability to absorb X-rays strongly. When engineered AuNPs are administered to a patient, they tend to accumulate in the tumor tissue. When an X-ray beam passes through the breast during a mammogram, the gold nanoparticles preferentially absorb more X-rays than the surrounding tissue. AuNPs appear as bright spots or areas of increased density on the mammogram. This differential absorption contrasts the tumor (where gold nanoparticles accumulate) and the healthy tissue (which absorbs fewer X-rays), making it easier for radiologists to identify and locate the tumor. The enhanced contrast provided by the gold nanoparticles can help radiologists detect smaller tumors or lesions that might be challenging to see on a standard mammogram, leading to a more accurate diagnosis of breast cancer (Chen *et al.*, 2020).

Conjugating ALA or MALA with AuNPs enables an increased selective uptake by cancer cells, due to the specific metabolism of ALA or MALA within these cells(Zhang *et al.*, 2015; Goncalves *et al.*, 2020). In cells incubated with ALAAu or MALAAu, the abundant PpIX production cannot be quickly converted to its final product, heme, and therefore accumulates within cells(Blanco *et al.*, 2015; Sachar *et al.*, 2016). The results shown in Fig. 3 confirm that ALA and MALA on the surface of NPs were metabolized to PpIX.

In the case of GABA-functionalized gold nanoparticles, since breast cancer cells have GABA receptors, GABA attached to the surface of the nanoparticles will be guided to bind specifically to receptors overexpressed in breast cancer cells. This targeted approach aims to increase the specificity and accuracy of mammographic imaging for breast cancer. This is the first time GABAAuNPs were synthesized and studied in cancer cells. The particles are stable and moderate stability.

The presence of gold nanoparticles has the potential to decrease the overall radiation dose required for breast cancer treatment, as demonstrated in studies by Nagi et al. (2017) and Torrisi et al. (2019) (Nagi *et al.*, 2017; Torrisi *et al.*, 2019). This reduction is achieved through the generation of reactive oxygen species (ROS) triggered by Auger electrons emitted from the gold nanoparticles. This is advantageous because it minimizes the risk of damage to healthy tissues. While the total radiation dose is lowered, the use of gold nanoparticles results in an increased radiation dose specifically targeted to the tumor site. The gold nanoparticles serve as enhancers or amplifiers of the radiation's effect at the tumor site, rendering it more lethal to cancer cells while preserving the integrity of surrounding healthy tissues.

PpIX can significantly increase the production of reactive oxygen species when exposed to X-ray irradiation(Takahashi *et al.*, 2013). PpIX absorption peak occurs around 380-430 nm. This range perfectly aligns with the Cherenkov radiation at 370-430 nm(Blum *et al.*, 2020; Yang *et al.*, 2022b). In the same way that occurs with photoirradiation, PpIX in the cells exposed to X-rays is excited from the singlet ground state to an excited singlet state, followed by intersystem crossing to an excited triplet state. The energy or electrons are transferred to oxygen molecules via type I and II reactions, generating reactive oxygen species (ROS), which causes cellular damage that leads to tumor cell death (Gutowski and Kowalczyk, 2013). In Cherenkov radiation-induced PDT (CR-PDT)(Cline *et al.*, 2019), X-rays for drug activation can treat deep tumors due to better tissue penetration than visible light.

ALA/MALAAuNPs was used in our experiment as radiosensitizers in CR-PDT or radiodynamic therapy(Yang *et al.*, 2022a). We demonstrated that ALA/MALAAuNPs reduced cell viability by around 20 % after 5 min of low-energy X-ray irradiation. In this case the ROS triggered by Auger electrons emitted from the gold nanoparticles was enhanced by ROS produced from PpIX excitation. For GABAAuNPs, only ROS triggered by Auger electrons emitted was achieved and decrease in cell viability was ~10%.

So, ALA, MALA and GABA gold nanoparticles can potentially be used as theranostic material enhancing diagnosis and cancer therapies, including radiodynamic therapy (ALA/MALAAu) and radiotherapy (GABAAu) for breast cancer. Figure 5 shows a diagram illustrating the procedures and potential uses of ALAAu, MALAAu, and GABAAuNPs.

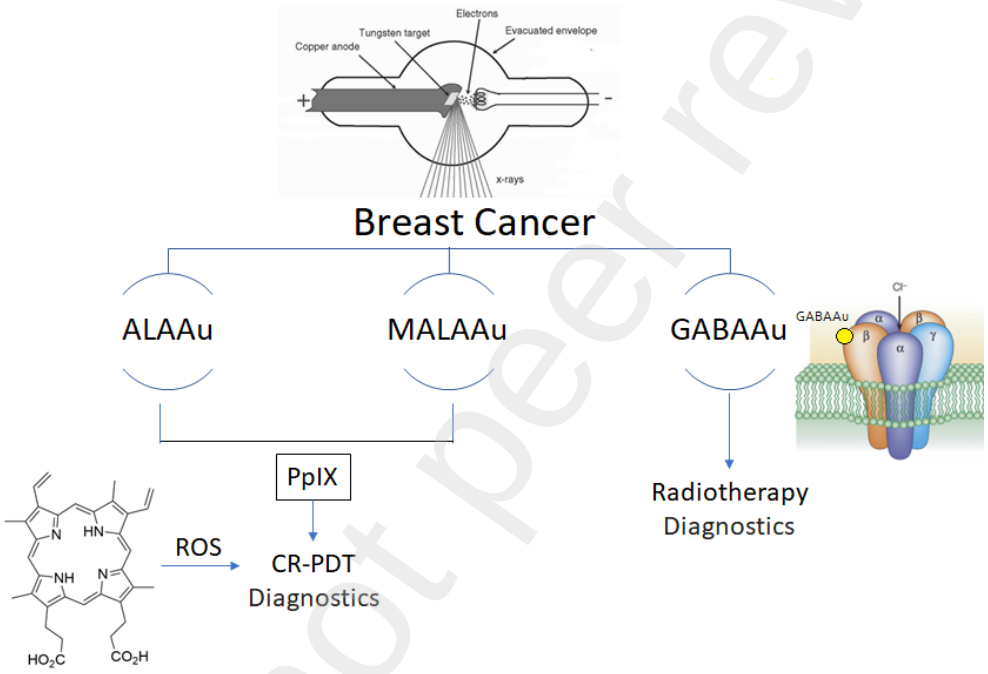

Figure 5. Diagram depicting processes and potential applications of ALAAu, MALAAu, and GABAAuNPs.

5. Conclusion

ALAAu, MALAAu and GABAAu nanoparticles were synthesized using the photoreduction process and exhibited excellent photophysical properties. Conjugation of ALA or MALA with nanoparticles allow their selective uptake by cancer cells due to the specific metabolism of ALA or MALA within these cells. Additionally, ALA/MALAAuNPs serve as radiosensitizers in Cherenkov radiation-induced PDT. GABAAuNPs can specifically bind to receptors overexpressed in breast cancer cells. When MCF-7 cells were incubated with ALAAuNPs and MALAAuNPs and then irradiated with 35 kV X-rays, there was a significant reduction in cell viability of approximately 22.9% and 18.7%, respectively, compared to non-irradiated cells. Incubation with GABAAuNPs resulted in a decrease in cell viability of about 9.7% compared to non-irradiated cells. These results indicate the potential of these nanoparticles to enhance breast cancer screening tests and radiotherapy.

Declaration of competing interest

The authors declare that they have no known competing financial interests or personal relationships that could have appeared to influence the work reported in this paper.

Acknowledgments

The authors would like to thank Multi-user Centers of ABC Federal University (UFABC), Energy and Nuclear Research Institute (IPEN/ CNEN-SP), The National Institute of Science and Technology ComplexFluids (INCT-FCX) grant 2014/50983-3.

6. References

Akram M, Iqbal M, Daniyal M and Khan A U 2017 Awareness and current knowledge of breast cancer *Biological Research* **50**

Akter Z, Khan F Z and Khan M A 2023 Gold Nanoparticles in Triple-Negative Breast Cancer Therapeutics *Current Medicinal Chemistry* **30** 316-34

Allen N C, Chauhan R, Bates P J and O'Toole M G 2022 Optimization of Tumor Targeting Gold Nanoparticles for Glioblastoma Applications *Nanomaterials* **12**

Amina S J and Guo B 2020 A Review on the Synthesis and Functionalization of Gold Nanoparticles as a Drug Delivery Vehicle *International Journal of Nanomedicine* **15** 9823-57

Bilynsky C, Millot N and Papa A L 2022 Radiation nanosensitizers in cancer therapy-From preclinical discoveries to the outcomes of early clinical trials *Bioengineering & Translational Medicine* **7**

Blanco K C, Moriyama L T, Inada N M, Salvio A G, Menezes P F C, Leite E J S, Kurachi C and Bagnato V S 2015 Fluorescence guided PDT for optimization of the outcome of skin cancer treatment *Frontiers in Physics* **3**

Blum N T, Zhang Y F, Qu J L, Lin J and Huang P 2020 Recent Advances in Self-Exciting Photodynamic Therapy *Frontiers in Bioengineering and Biotechnology* **8**

Brzozowska A, Burdan F, Duma D, Solski J and Mazurkiewicz M 2017 gamma-amino butyric acid (GABA) level as an overall survival risk factor in breast cancer *Annals of Agricultural and Environmental Medicine* **24** 435-9

Chen X Y, Yung L Y L, Tan P H and Bay B H 2022 Harnessing the Immunogenic Potential of Gold Nanoparticle-Based Platforms as a Therapeutic Strategy in Breast Cancer Immunotherapy: A Mini Review *Frontiers in Immunology* **13**

Chen Y, Yang J, Fu S Z and Wu J B 2020 Gold Nanoparticles as Radiosensitizers in Cancer Radiotherapy *International Journal of Nanomedicine* **15** 9407-30

Cline B, Delahunty I and Xie J 2019 Nanoparticles to mediate X-ray-induced photodynamic therapy and Cherenkov radiation photodynamic therapy *Wiley Interdisciplinary Reviews-Nanomedicine and Nanobiotechnology* **11**

Diffey J 2017 How many physicists does it take to test a mammography unit? *Australasian Physical & Engineering Sciences in Medicine* **40** 1-6

Fathy M M, Mohamed F S, Elbialy N and Elshemey W M 2018 Multifunctional Chitosan-Capped Gold Nanoparticles for enhanced cancer chemo-radiotherapy: An invitro study *Physica Medica-European Journal of Medical Physics* **48** 76-83

Goncalves K D, da Silva M N, Sicchieri L B, Silva F R D, de Matos R A and Courrol L C 2015 Aminolevulinic acid with gold nanoparticles: a novel theranostic agent for atherosclerosis *Analyst* **140** 1974-80

Goncalves K D, Vieira D P, Levy D, Bydlowski S P and Courrol L C 2020 Uptake of silver, gold, and hybrids silver-iron, gold-iron and silver-gold aminolevulinic acid nanoparticles by MCF-7 breast cancer cells *Photodiagnosis and Photodynamic Therapy* **32**

Goncalvez K D, Vieira D P and Courrol L C 2018 STUDY OF THP-1 MACROPHAGE VIABILITY AFTER SONODYNAMIC THERAPY USING METHYL ESTER OF 5-AMINOLEVULINIC ACID GOLD NANOPARTICLES *Ultrasound in Medicine and Biology* **44** 2009-17

Gutowski M and Kowalczyk S 2013 A study of free radical chemistry: their role and pathophysiological significance *Acta Biochimica Polonica* **60** 1-16

Hon J D C, Singh B, Sahin A, Du G, Wang J H, Wang V Y, Deng F M, Zhang D Y, Monaco M E and Lee P 2016 Breast cancer molecular subtypes: from TNBC to QNBC *American Journal of Cancer Research* **6** 1864-72

Hsu J C, Nieves L M, Betzer O, Sadan T, Noel P B, Popovtzer R and Cormode D P 2020 Nanoparticle contrast agents for X-ray imaging applications *Wiley Interdisciplinary Reviews-Nanomedicine and Nanobiotechnology* **12**

Janssen S, Kasmann L, Fahlbusch F B, Rades D and Vordermark D 2018 Side effects of radiotherapy in breast cancer patients The Internet as an information source *Strahlentherapie Und Onkologie* **194** 136-42

Lebron-Zapata L and Jochelson M S 2018 Overview of Breast Cancer Screening and Diagnosis *Pet Clinics* **13** 301-+

Lorente-Ramos R M and Arman J A 2022 Review of Contrast-Enhanced Mammography *Contemporary Diagnostic Radiology* **45**

Mateus J E, Valdivieso W, Hernandez I P, Martinez F, Paez E and Escobar P 2014 Cell accumulation and antileishmanial effect of exogenous and endogenous protoporphyrin IX after photodynamic treatment *Biomedica* **34** 589-97

Nagi N M S, Khair Y A M and Abdalla A M E 2017 Capacity of gold nanoparticles in cancer radiotherapy *Japanese Journal of Radiology* **35** 555-61

Noor F, Noor A, Ishaq A R, Farzeen I, Saleem M H, Ghaffar K, Aslam M F, Aslam S and Chen J T 2021 Recent Advances in Diagnostic and Therapeutic Approaches for Breast Can- cer: A Comprehensive Review *Current Pharmaceutical Design* **27** 2344-65

Perry H, Phillips J, Dialani V, Slanetz P J, Fein-Zachary V J, Karimova E J and Mehta T S 2019 Contrast-Enhanced Mammography: A Systematic Guide to Interpretation and Reporting *American Journal of Roentgenology* **212** 222-31

Sachar M, Anderson K E and Ma X C 2016 Protoporphyrin IX: the Good, the Bad, and the Ugly *Journal of Pharmacology and Experimental Therapeutics* **356** 267-75

Schulz-Wendtland R, Wenkel E, Wacker T and Hermann K P 2009 Quo vadis? Trends in Digital Mammography *Geburtshilfe Und Frauenheilkunde* **69** 108-17

Swaminathan H, Saravanamurali K and Yadav S A 2023 Extensive review on breast cancer its etiology, progression, prognostic markers, and treatment *Medical Oncology* **40**

Takahashi J, Misawa M, Murakami M, Mori T, Nomura K and Iwahashi H 2013 5-Aminolevulinic acid enhances cancer radiotherapy in a mouse tumor model *Springerplus* **2**

Torrisi L, Restuccia N and Torrisi A 2019 Study of gold nanoparticles for mammography diagnostic and radiotherapy improvements *Reports of Practical Oncology and Radiotherapy* **24** 450-7

Wu L, Zhang Y, Zheng C L, Zhao F Q and Lin Y 2023 Gamma-Aminobutyric Acid Type A Receptor Subunit Delta (GABRD) Inhibits Breast Cancer Progression by Regulating the Cell Cycle *Iranian Journal of Public Health* **52** 542-52

Yang D, Cvetkovic D, Dos Santos T, Chen L and Ma C 2022a Efficacy and Photon Energy Dependency of In-Vivo Radiodynamic Therapy (RDT) with 5-Aminolevulinic Acid (5-ALA) *Medical Physics* **49** E250-E1

Yang D M, Cvetkovic D, Chen L L and Ma C M C 2022b Therapeutic effects of in-vivo radiodynamic therapy (RDT) for lung cancer treatment: a combination of 15MV photons and 5-aminolevulinic acid (5-ALA) *Biomedical Physics & Engineering Express* **8**

Yang L P, Zhu J, Wang L L, He L B, Gong Y and Luo Q F 2023 A novel risk score model based on gamma-aminobutyric acid signature predicts the survival prognosis of patients with breast cancer *Frontiers in Oncology* **13**

Zhang Z X, Wang S J, Xu H, Wang B and Yao C P 2015 Role of 5-aminolevulinic acid-conjugated gold nanoparticles for photodynamic therapy of cancer *Journal of Biomedical Optics* **20** 8